Velocity Profiling of Two-phase Flows Based on Soft-Field Volume Tomography

Shah M. Chowdhury, Rafiul K. Rasel, Fernando L. Teixeira
Department of Electrical and Computer Engineering
The Ohio State University
Columbus, OH 43212, USA
chowdhury.79@osu.edu, rasel.1@osu.edu, teixeira.5@osu.edu

Qussai M. Marashdeh
Tech4Imaging LLC
Columbus, OH 43220, USA
marashdeh@tech4imaging.com

***Abstract*—In this paper, a soft-field tomography-based velocity profile reconstruction is conducted for different two-phase flow models. The method is based on the use of the sensor sensitivity gradient in the region of interest based on a Laplacian interrogating field. The described method offers a robust and reliable velocity profile measurement over earlier cross-correlation-based methods.**

I. INTRODUCTION

Multiphase flows are very common in industrial and scientific settings. A popular direct method for two-phase flows is volume fraction measurement based on electrical capacitance sensors [1]–[3]. In particular, electrical capacitance volume tomography (ECVT) is a relatively new soft-field tomography technique that is highly suited for direct three-dimensional (3D) measurement in harsh environments of two-phase flow measurement exhibiting different permittivity ε for each phase [4]. In ECVT, a multi-electrode capacitance sensor is mounted on a flow pipe and the mutual capacitance between the electrode pairs is obtained (denoted as a frame). In this modality, the interrogating field has a Laplacian nature and measurement results are scale-invariant under certain limits. This measurement is used to reconstruct the permittivity distribution inside the region of interest (RoI) [5]. Such information may be used as aid to interpretation of various quantities of interest such as volume fraction, liquid holdup etc. [6].

A velocity profile is another volumetric quantity of interest, consisting of the spatial map of the velocity vector field inside the RoI. ECVT has been successfully applied for velocity profile measurement based on temporal changes in the measured capacitance frames [7]. Here, we illustrate this methodology towards velocity profiling of two complementary flow scenarios: (*i*) a high permittivity moving object in low permittivity background, e.g. solid-in-gas, and (*ii*) a low permittivity moving object in high permittivity background, e.g. gas-in-oil.

II. METHODOLOGY

Fig. 1 shows a typical ECVT sensor. The electrodes are activated with a low-frequency (around 500 kHz) excitation, resulting in the quasi-static (Laplacian) conditions, described by Gauss's law as $\vec{\nabla}\cdot\left(\varepsilon\vec{\nabla}\phi\right)=0$, where ε is the permittivity distribution and ϕ is the electric potential. For capacitance

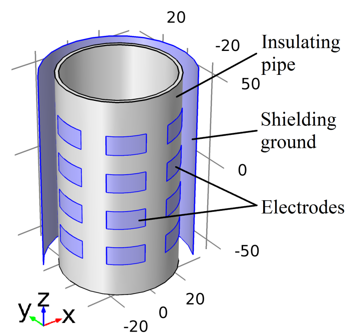

Fig. 1. A 24-electrode capacitance sensor arranged in a 6×4 configuration. Dimension are in mm.

measurements, the sensor can be treated as an n-port reciprocal device having $M=\binom{n}{2}=n(n-1)/2$ number of independent measurements. Therefore, a capacitance frame $\boldsymbol{C}$ can be considered as an $M\times1$ vector. For imaging, the sensor domain is discretized into small volume elements, or voxels. Each voxel is assigned a permittivity g and velocity vector (v_x,v_y,v_z), which can be collectively written as $N\times1$ vectors $\boldsymbol{g}$ and $(\boldsymbol{v}_x,\boldsymbol{v}_y,\boldsymbol{v}_z)$ for N number of voxels. Fig. 2 shows an outline for the image and velocity reconstruction based on successive measurement frames $\boldsymbol{C}_1,\boldsymbol{C}_2,\boldsymbol{C}_3,\ldots$ etc. The reconstruction is essentially an inverse problem [8] involving the $M\times N$ sensor sensitivity matrix $\boldsymbol{S}$ and the sensitivity gradient matrices $(\boldsymbol{F}_x,\boldsymbol{F}_y,\boldsymbol{F}_z)$ respectively [7], [9], [10]. Usually, Landweber iteration method is used for image reconstruction, whereas linear back projection (LBP) is used for velocity reconstruction [11].

III. RESULTS

Fig. 3a shows the simulation setup for two high permittivity solid objects moving in low permittivity gas background with an average velocity $\vec{v}=2$ mm/s. The corresponding reconstructed velocity profile is shown in Fig. 3b, based on a parallel normalization [12]. Fig. 4a shows the simulation setup for two low permittivity gas objects moving in high permittivity oil background with an average velocity $\vec{v}=2$ mm/s. The corresponding reconstructed velocity profile is shown in Fig. 4b, based on an inverse parallel normalization [12]. The reconstructed profiles match well the true velocity $\vec{v}$.

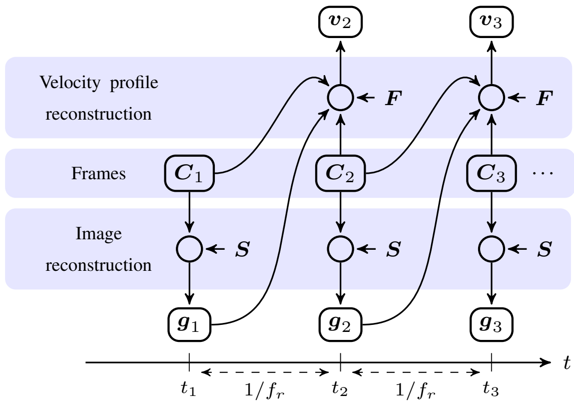

Fig. 2. Method for successive image and velocity reconstruction. Symbols used, $\boldsymbol{C}$: capacitance vector, $\boldsymbol{g}$: image vector, $\boldsymbol{v}$: velocity profile vectors $(\boldsymbol{v}_x, \boldsymbol{v}_y, \boldsymbol{v}_z)$, $\boldsymbol{S}$: sensitivity matrix, $\boldsymbol{F}$: sensitivity gradient matrices $(\boldsymbol{F}_x, \boldsymbol{F}_y, \boldsymbol{F}_z)$, t: time, and f_r: frame rate.

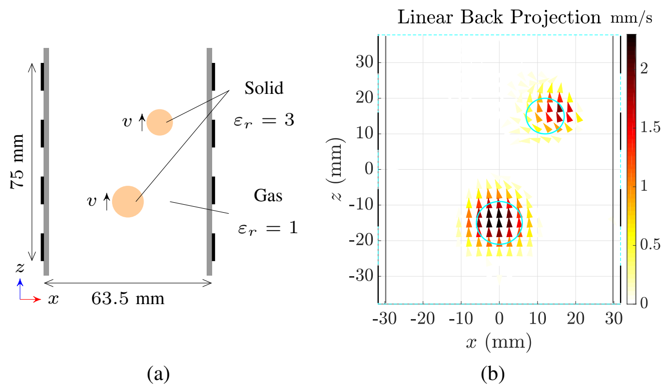

Fig. 3. Simulation results for high permittivity solid objects moving in low permittivity gas background. (a) Simulation setup with $v = 2$ mm/s. (b) Reconstructed velocity profile.

Possible extensions for this method would be the application of synthetic or adaptive electrodes for accuracy enhancement [13], combination with displacement-current phase measurement based techniques [14], and utilization of multi-frequency acquisition based techniques for three-phase flow measurements [15], [16]. We note that a limitation of the described velocity profiling method is that it is unable to detect velocity in the background (continuous) phase since this phase does not cause any signal variation.

Acknowledgment

This work is supported by NASA Space Technology Mission Directorate grant NNX16CC10C, and by the DOE grants DE-SC0011936 and DE-SC0010228.

References

[1] A. Jaworek, A. Krupa, and M. Trela, "Capacitance sensor for void fraction measurement in water/steam flows," *Flow Meas. Instrum.*, vol. 15, no. 5-6, pp. 317–324, Oct.-Dec. 2004.

[2] Z. Cui, H. Wang, Z. Chen, Y. Xu, and W. Yang, "A high-performance digital system for electrical capacitance tomography," *Meas. Sci. Technol.*, vol. 22, no. 5, p. 055503, 2011.

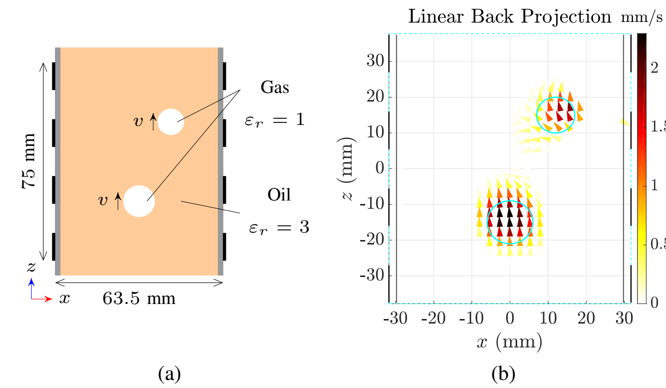

Fig. 4. Simulation results for low permittivity gas objects moving in high permittivity oil background. (a) Simulation setup with $v = 2$ mm/s. (b) Reconstructed velocity profile.

[3] R. K. Rasel, C. Gunes, Q. M. Marashdeh, and F. L. Teixeira, "Exploiting the Maxwell-Wagner-Sillars effect for Displacement-Current Phase Tomography of two-phase flows," *IEEE Sensors J.*, vol. 17, no. 22, pp. 7317–7324, Nov. 2017.

[4] F. Wang, Q. Marashdeh, L.-S. Fan, and W. Warsito, "Electrical Capacitance Volume Tomography: Design and applications," *Sensors*, vol. 10, no. 3, pp. 1890–1917, Mar. 2010.

[5] Q. M. Marashdeh, F. L. Teixeira, and L.-S. Fan, "Electrical capacitance tomography," in *Industrial Tomography: Systems and Applications*, 1st ed., M. Wang, Ed. Cambridge, UK: Woodhead/Elsevier, 2015, ch. 1, pp. 3–21.

[6] A. Wang, Q. Marashdeh, B. J. Motil, and L.-S. Fan, "Electrical capacitance volume tomography for imaging of pulsating flows in a trickle bed," *Chem. Eng. Sci.*, vol. 119, pp. 77–87, Nov. 2014.

[7] S. Chowdhury, Q. M. Marashdeh, and F. L. Teixeira, "Velocity profiling of multiphase flows using capacitive sensor sensitivity gradient," *IEEE Sensors J.*, vol. 16, no. 23, pp. 8365–8373, Dec. 2016.

[8] J. Ye, H. Wang, and W. Yang, "Image reconstruction for electrical capacitance tomography based on sparse representation," *IEEE Trans. Instrum. Meas.*, vol. 64, no. 1, pp. 89–102, Jan. 2015.

[9] Q. M. Marashdeh and F. L. Teixeira, "Sensitivity matrix calculation for fast 3-D electrical capacitance tomography (ECT) of flow systems," *IEEE Trans. Magn.*, vol. 40, no. 2, pp. 1204–1207, Mar. 2004.

[10] W. Fang, "A nonlinear image reconstruction algorithm for electrical capacitance tomography," *Meas. Sci. Technol.*, vol. 15, no. 10, p. 2124, Sep. 2004.

[11] S. Chowdhury, C. Gunes, Q. M. Marashdeh, and F. L. Teixeira, "Fast imaging of velocity profiles of two-phase flows using electrical capacitance volume tomography sensors," in *2017 XXXIInd URSI GASS*, Montreal, QC, Canada, Aug. 2017, pp. 1–3.

[12] S. Chowdhury, Q. M. Marashdeh, and F. L. Teixeira, "Inverse normalization method for cross-sectional imaging and velocimetry of two-phase flows based on Electrical Capacitance Tomography," *IEEE Sensors Lett.*, vol. 2, no. 1, pp. 1–4, Mar. 2018.

[13] Q. M. Marashdeh, F. L. Teixeira, and L.-S. Fan, "Adaptive electrical capacitance volume tomography," *IEEE Sensors J.*, vol. 14, no. 4, pp. 1253–1259, Apr. 2014.

[14] C. Gunes, Q. M. Marashdeh, and F. L. Teixeira, "A comparison between electrical capacitance tomography and displacement-current phase tomography," *IEEE Sensors J.*, vol. 17, no. 24, pp. 8037–8046, Dec. 2017.

[15] R. K. Rasel, C. E. Zuccarelli, Q. M. Marashdeh, L.-S. Fan, and F. L. Teixeira, "Toward multiphase flow decomposition based on electrical capacitance tomography sensors," *IEEE Sensors J.*, vol. 17, no. 24, pp. 8027–8036, Dec. 2017.

[16] M. Zhang and M. Soleimani, "Simultaneous reconstruction of permittivity and conductivity using multi-frequency admittance measurement in electrical capacitance tomography," *Meas. Sci. Technol.*, vol. 27, no. 2, Feb. 2016.